The ATLAS muon Micromegas R&D project: towards large-size chambers for the s-LHC

The ATLAS muon Micromegas R&D project: towards large-size chambers for the s-LHC

T. Alexopoulos,[a] **A.A. Altintas,**[b] **M. Alviggi,**[c] **M. Arik,**[b] **S.A. Cetin,**[d] **V. Chernyatine,**[e]
E. Cheu,[f] **D. Della Volpe,**[c] **M. Dris,**[a] **D. Fassouliotis,**[g] **E.N. Gazis,**[a] **R. Giordano,**[c]
V. Gratchev,[h] **L. Guan,**[i] **P. Iengo,**[j] **P. Ioannou,**[g] **C. Li,**[i] **K. Johns,**[f] **V. Kaushik,**[f]
A. Khodinov,[k] **C. Kourkoumelis,**[g] **S. Maltezos,**[a] **K. Mermigka,**[a] **H. Müller,**[l]
K. Nikolopoulos,[g,e,1] **W. Park,**[m] **S. Persembe,**[b] **C. Petridou,**[n] **R. Petti,**[m]
V. Polychronakos,[e] **M.V. Purohit,**[m] **D. Sampsonidis,**[n] **G. Sekhniaidze,**[c] **M. Shao,**[i]
Y.J. Sun,[i] **G. Tsipolitis,**[a] **R. Veenhof,**[o] **X.L. Wang,**[i] **J. Wotschack,**[l] **S.X. Wu,**[i] **T. Zhao**[p]
and Z.G. Zhao[i]

[a]*National Technical University of Athens,*
Zografou Campus, Athens, 15780, Greece

[b]*Bogazici University of Istanbul,*
Bebek/Istanbul, 34342, Turkey

[c]*University of Naples,*
Naples, 80126, Italy

[d]*Dogus University of Istanbul,*
Istanbul, 34722, Turkey

[e]*Brookhaven National Laboratory,*
Upton, NY 11973, U.S.A.

[f]*University of Arizona,*
Tucson, AZ 85721, U.S.A.

[g]*University of Athens,*
Ilissia, 15771, Greece

[h]*Petersburg Nuclear Physics Institute,*
Gatchina, 188350, Russia

[i]*University of Science and Technology of China,*
An Hui, 230026, People's Republic of China

[1]Corresponding author

^{j}*LAPP, CNRS/IN2P3,*
  Annecy-le-Vieux, F-74941, France
^{k}*Stony Brook University,*
  Stony Brook, NY 11794-3800, U.S.A.
^{l}*CERN,*
  Geneve, CH-1211, Switzerland
^{m}*University of South Carolina,*
  Columbia, SC 29208, U.S.A.
^{n}*University of Thessaloniki,*
  Thessaloniki, 54124, Greece
^{o}*University of Wisconsin,*
  Madison, WI 53706-1481, U.S.A.
^{p}*University of Washington,*
  Seattle, WA 98195, U.S.A.

E-mail: konstantinos.nikolopoulos@cern.ch

ABSTRACT: Detectors based on the bulk-Micromegas technology exhibit position resolution better than $100\,\mu$m at counting rates of up to several tens of kHz/cm^2, along with trigger capabilities. These characteristics, combined with the detector's mechanical robustness and the possibility for cost-effective industrial production, makes them a promising candidate for the ATLAS Muon Spectrometer upgrade in a future luminosity enhancement of the LHC. The R&D project status will be presented together with the obtained results in the effort to define the baseline system specifications.

Contents

1   Introduction

The ATLAS detector [1, 2] is designed to exploit the full physics potential of the Large Hadron Collider (LHC) [3] which will provide pp collisions at $\sqrt{s} = 14\,\text{TeV}$ with an instantaneous luminosity of $10^{34}\,\text{cm}^{-2}\text{s}^{-1}$. A major design consideration was the requirement for a Muon Spectrometer [4] providing high quality stand-alone muon identification and momentum measurement, along with trigger capabilities and extended pseudorapidity (η) coverage. To this end, a system of three superconducting air-core toroids is employed in combination with high spatial resolution tracking chambers — Monitored Drift Tubes and Cathode Strip Chambers — and fast trigger detectors — Resistive Plate Chambers and Thin Gap Chambers. These detectors are able to sustain counting rates at least up to five times the expected rates at nominal LHC luminosity. The corresponding counting rates are summarized in figure 1.

For the future, an upgraded LHC — the super LHC (s-LHC) — delivering ten times higher instantaneous luminosity is being considered. This increase in luminosity would result in a roughly proportional increase of the expected counting rates from muons and background sources, namely photons, neutrons and protons. For the detector coverage and the good detector performance to be maintained under these conditions, it is likely that an upgrade of the present tracking and trigger chambers in the forward region, $|\eta| > 2$, will be necessary. Specifically, this applies to the Inner and Middle stations of the End-Cap Muon Spectrometer corresponding to a total surface of $400\,\text{m}^2$.

The Micromegas (MICROMEsh GAseous Structure) detector [6, 7] provides excellent position resolution and high counting rate performance, which can be combined with trigger capabilities. The bulk-Micromegas technology [8] provides the possibility to produce mechanically robust large-size detectors with cost-effective industrial processes. Thus, the bulk-Micromegas is a promising candidate for the upgrade of the ATLAS Muon Spectrometer at the s-LHC.
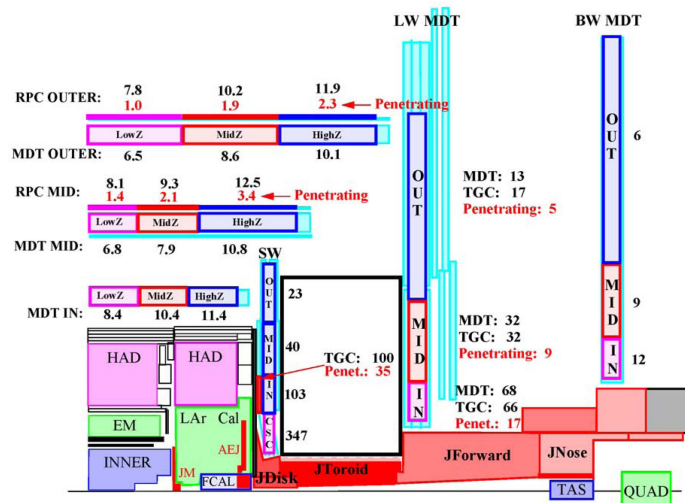
Figure 1. Average single plane counting rates in Hz/cm^2 at the nominal LHC luminosity, 10^{34} cm^{-2}s^{-1}, in the various parts of the Muon Spectrometer, from [5].

2 The R&D project: muon ATLAS Micromegas activity

The currently available estimates of the expected counting rates are plagued with large uncertainties and thus a solid definition of the performance requirements for the s-LHC is not possible. This situation will improve as soon as the LHC provides us with its first collisions, and the counting rates owing to muons and background will be measured. Nevertheless, using the currently available information, a set of performance requirements serving as guideline to the R&D effort has been established:

- High counting rate capability, $> 20\,\text{kHz/cm}^2$, including dense ionization

- High single plane detection efficiency, $\gtrsim 98\%$

- Good spatial resolution, $\approx 100\,\mu\text{m}$, possibly up to large incident angles, $< 45^o$

- Second coordinate measurement

- Two-track separation at distance of ≈ 1–2 mm

- Good time resolution, $\approx 5\,\text{ns}$, to allow bunch crossing identification

- Level-1 triggering capability

- Good aging properties

These detector requirements should be coupled with appropriate read-out electronics which will be able to cope with trigger rates of the order of 100 kHz, providing good pulse amplitude and timing measurements. Moreover, the limited bandwidth of the read-out link requires on-board zero-suppression functionality. For reliable operation in the harsh radiation environment of ATLAS radiation hardness and high single-event-upset tolerance are of primary importance.
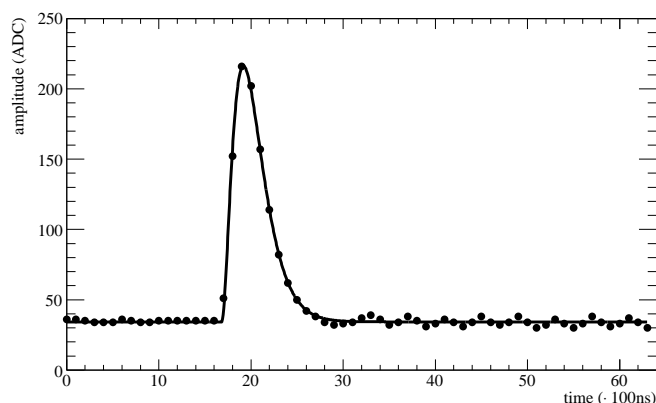
Figure 2. Electronics response for a δ pulse, sampled every 100 ns. The solid line is a fit to the design shaper response. One ADC count corresponds roughly to 900 electrons.

Although Micromegas detectors have been in wide use already for over a decade, they have not yet operated in colliding beam experiment. The Muon ATLAS Micromegas R&D project has been launched in 2007 aiming to use the bulk-Micromegas technology to produce large-size chambers (about $1\,\text{m} \times 2\,\text{m}$) complying with the above mentioned requirements.

3 Medium-size prototype beam test 2008

In 2007 a medium-size bulk-Micromegas with an active area of $450\,\text{mm} \times 350\,\text{mm}$ was produced by CERN/EN-ICE. At the time of its production, it was one of the largest bulk-Micromegas ever built. The mesh was formed by woven stainless steel wires arranged at a pitch of $78\,\mu\text{m}$. The wire diameter was $25\,\mu\text{m}$. The amplification gap was $128\,\mu\text{m}$ thick, while the drift gap was adjusted to 5 mm. The copper read-out electrodes where shaped in strips and arranged in groups with different pitch — 250, 500, 1000 and 2000 μm — and length — 450 and 225 mm. The conditioning of the chamber took place at CERN and its performance was first studied using an ^{55}Fe radioactive source. A detailed description of the chamber construction and preliminary tests can be found in [9].

The prototype chamber was then exposed to 120 GeV pions at the CERN H6 beam line during the summer of 2008. 32 strips of the prototype were connected to charge sensitive preamplifiers (CSP) with a voltage/charge conversion of 2 mV/fC, followed by electronics cards [10] with shapers of 200 ns peaking time and with a signal gain of 3.7 in the high gain channels and 0.23 in the corresponding low gain channels. The CSPs were efficiently spark protected via cross-coupled diodes and capacitive coupling. The shaper signals were digitized by 10 bit ALTRO chips [11] at a sampling frequency of 10 MHz with a trigger pipeline of 16 events and 64 samples per event. The data were recorded by the DATE system [12]. An example of the output signal for a single channel is presented in figure 2.

The experimental set-up is presented in figure 3. The beam entered from the back of the photograph, passed through the Micromegas and subsequently through the set-up of scintillators and Si detectors. The trigger was defined by the coincidence of scintillators 1 and 2. Beam halo events were rejected by a third scintillator with a 3 cm diameter hole at the beam position used as a veto. This latter scintillator, which is not shown in figure 3, was positioned 50 cm downstream of
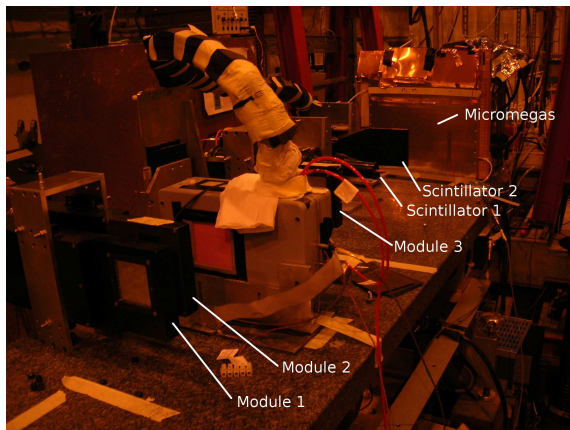
Figure 3. The 2008 beam test set-up. The Micromegas prototype, the Si telescope modules and the trigger scintillators are indicated.
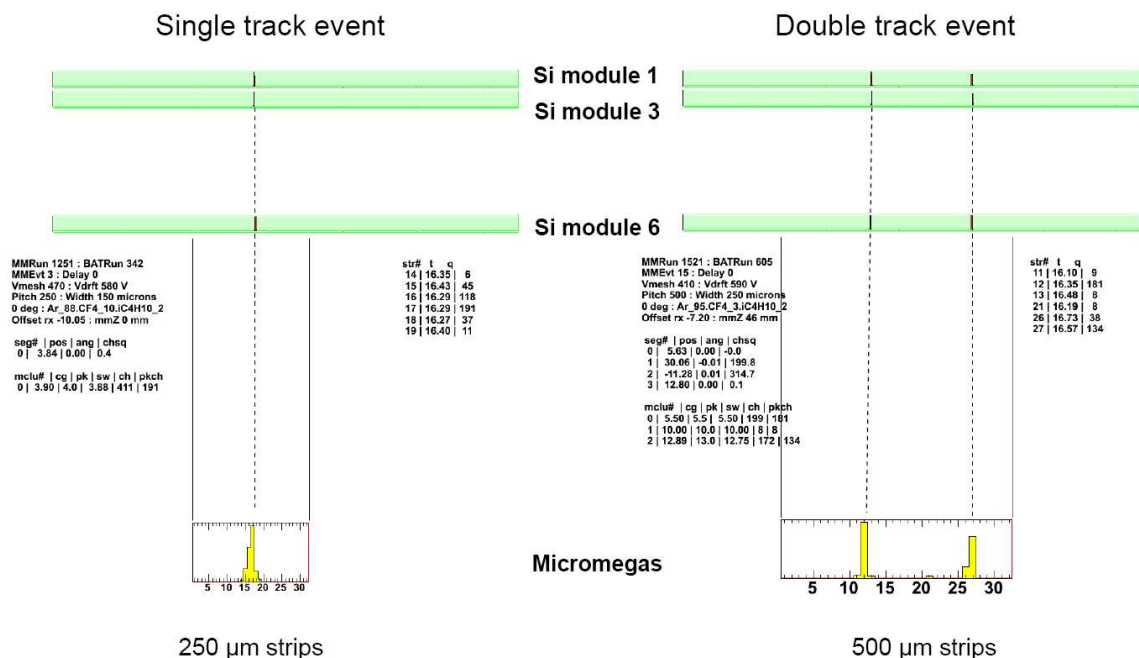

Figure 4. Event displays from the 2008 beam test. On the left, a single track, and on the right, a double track event is presented.

silicon Module 1. An external reference measurement on the plane normal to the beam direction was given by a telescope consisting of three modules of silicon strip detectors [13]. The point resolution of each module was estimated to be 7.7 μm.

During the beam test, three different gas mixtures were used — Ar:CO$_2$:iC$_4$H$_{10}$ (88:10:2), Ar:CF$_4$:iC$_4$H$_{10}$ (88:10:2) and Ar:CF$_4$:iC$_4$H$_{10}$ (95:3:2) — and data where collected with different strip pitches and incident track angles. In figure 4 (left) a display of a single track event is presented. The hits on the telescope modules are depicted at the upper part of the figure. At the lower part of the figure, the signals on the 32 strips of the Micromegas are presented. The strip pitch used is
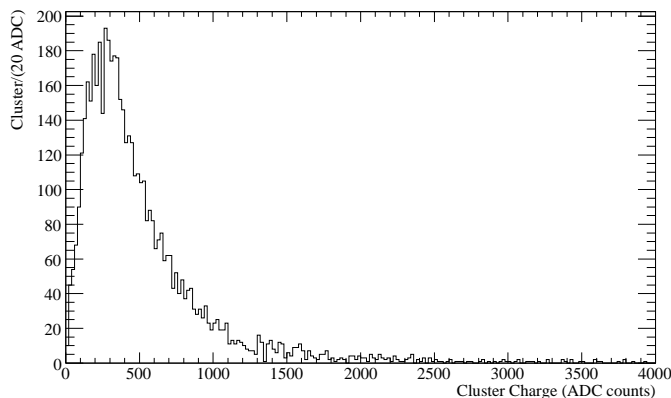
Figure 5. Cluster charge distribution for pions of $120\,\mathrm{GeV}$ in $\mathrm{Ar:CF_4:iC_4H_{10}}$ (88:10:2). The amplification field was $37\,\mathrm{kV/cm}$, while the drift field was $220\,\mathrm{V/cm}$.

$250\,\mu\mathrm{m}$. The formation of a charge cluster, with most of the charge being collected in two strips, is visible. On the right part of figure 4, the corresponding display for an event with two tracks on $500\,\mu\mathrm{m}$ strips is shown. In figure 5, the distribution of the total cluster charge is presented for $\mathrm{Ar:CF_4:iC_4H_{10}}$ (88:10:2).

The position of the particle is reconstructed by charge interpolation in the cluster. The width of the charge distribution was found to be $\approx 280\,\mu\mathrm{m}$ full-width at half-maximum. The spatial resolution is determined from the difference between the position measured in the Micromegas and the extrapolation of the telescope track to the Micromegas. The width of this distribution is affected by two contributions a) the intrinsic Micromegas resolution; and b) the uncertainty of the track extrapolation. The latter is due to the intrinsic resolution of the telescope and the multiple scattering in the trigger scintillators located between the Micromegas detector and the telescope. It was estimated to be $(61 \pm 2)\,\mu\mathrm{m}$, where the attributed uncertainty is systematic arising from the imprecise knowledge of the amount of material in the scintillators.

In figure 6(a) and 6(b), the corresponding distributions are presented for a Micromegas strip pitch of $250\,\mu\mathrm{m}$ and $500\,\mu\mathrm{m}$ respectively, for normal incidence. The estimated spatial resolution of the Micromegas detector, $\sigma_{\mathrm{Micromegas}}$, is:

$$\sigma_{\mathrm{Micromegas}} = (24 \pm 7)\mu\mathrm{m} \text{ for } 250\mu\mathrm{m} \text{ strip pitch}$$
$$\sigma_{\mathrm{Micromegas}} = (36 \pm 5)\mu\mathrm{m} \text{ for } 500\mu\mathrm{m} \text{ strip pitch}$$

The relative uncertainties in these estimates are 30% and 15% for 250 and $500\,\mu\mathrm{m}$ strip widths respectively and, moreover, they are correlated in the two measurements. This is due to the dominance of the reference measurement extrapolation uncertainty on the width of the difference between the Micromegas and the reference position measurement. The accuracy of the extrapolation uncertainty estimate in the set-up is defined by the knowledge of the amount of material between the silicon telescope and the Micromegas, which is only known at the 10% level. Although every effort to account for this oversight has been made, the magnitude and the nature of the uncertainty makes the above quoted resolutions more an order of magnitude estimate rather than a precise characterisation of the chamber performance.

The corresponding hit reconstruction efficiency, was estimated to be $\approx 99\%$. The observed inefficiency was found to be spatially correlated with the positions of the micromesh support pillars.
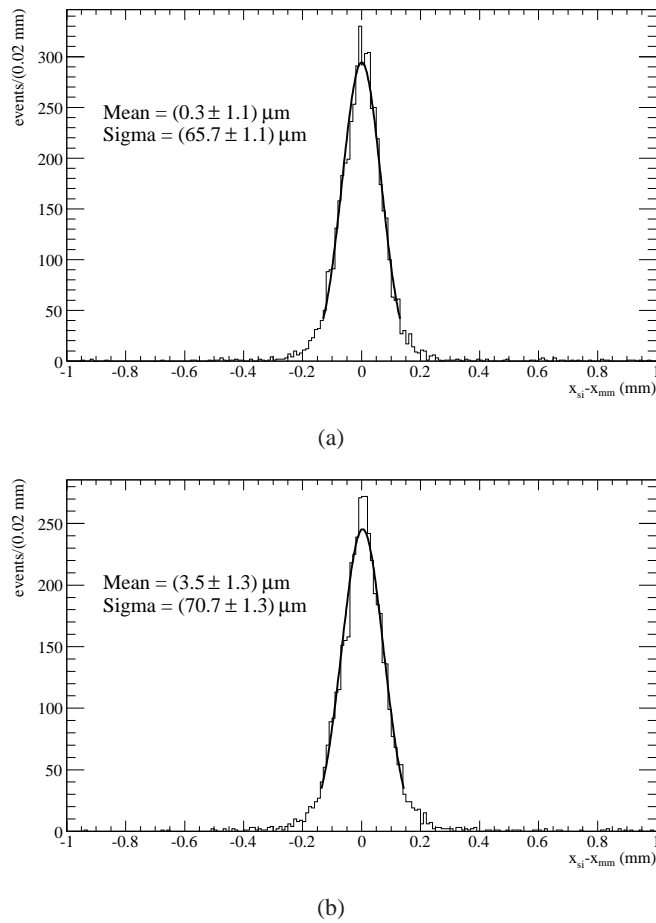
(a)

(b)

Figure 6. Difference between the position measured by the Micromegas and the extrapolated telescope track, for (a) 250 μm and (b) 500 μm strip pitch.

4 Micromegas simulation

In order to improve the understanding of the beam test results, to ease performance studies for different operation parameters choice and to evaluate the potential of new ideas, it was deemed useful to develop a simulation of the detector, starting from the microscopic processes in the gas up to the output of the electronics.

For the development of this simulation suite established simulation codes have been used as much as possible. The drift part is handled by GARFIELD [14] which interfaces HEED [15] for the modeling of ionization processes in the gas and Magboltz [16] for the transport properties of the drifting electrons. The amplification and electronics part is handled by custom code, which uses a semi-analytical method for the ion induced charge calculation [17]. The simulation has been configured to resemble the beam test set-up.

In figure 7, a simulated event is shown for a strip width of 500 μm and a drift gap of 5 mm. For clarity only the central strip (right) and its neighbour with the highest charge (left) are shown.
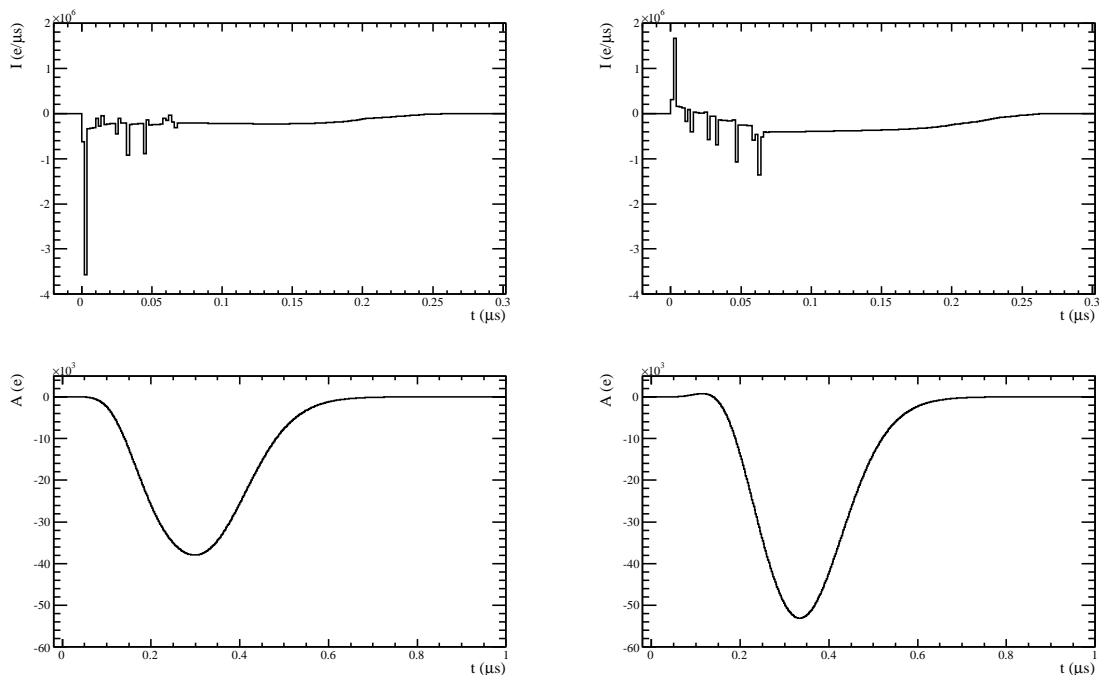
Figure 7. A simulated event for a strip width of $500\,\mu$m. Only the central (right) and the neighbour strip with the largest charge (left) are presented. On the upper row, the current developed in the amplification gap is depicted. In the lower row, the shaper output is presented. Note the different time scales in the two rows.

In the upper row, the current developed in the amplification gap is presented as a function of time. The spikes correspond to the arrival of the electron clusters. It can be seen that several electrons are collected in the neighbouring strip indicating that the track passed near the boundary of the two strips. The long current tail induced by the ion drift is also clearly visible. In the lower row the shaper output is presented.

In figure 8, the difference between the reconstructed and the true position of the simulated track is presented for four different strip sizes. The performance deteriorates with increasing strip width and non-gauss tails are observed. It should be noted that the events in the tails are mainly cases where the incident particle passed through the center of the strip. In these cases, due to the large strip width, not enough charge for reliable interpolation is deposited in the neighbouring strips.

In figure 9, the spatial resolution obtained from the beam test data and the simulation is directly compared and found to be in good agreement. It is reminded, section 3, that the uncertainties on the experimental measurements are correlated.

The dependence of the position resolution on the incidence angle is shown in figure 10. Four different strip widths are used, along with two different reconstruction algorithms: charge interpolation and binary read-out. In the latter, the geometrical mean of the strips exceeding a certain threshold — in this particular case 5 times the electronic noise — is used. The charge interpolation method provides superior results for small incidence angles, while the binary read-out method is found to be more stable. The improvement in position resolution with increasing incidence angle observed for the charge interpolation at $1000\,\mu$m strip width could be attributed to better charge sharing, exactly due to the track inclination, which resolves the left-right ambiguity for tracks passing near the center of the strip.
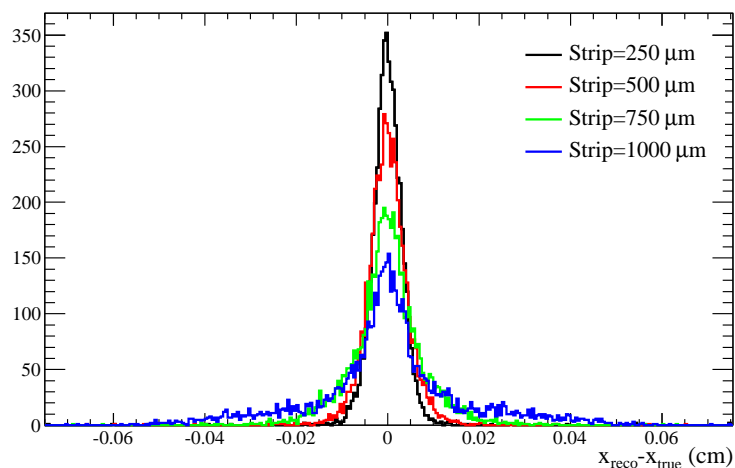
– 7 –

Figure 8. Simulated residual distribution for uniform illumination and different strip widths.
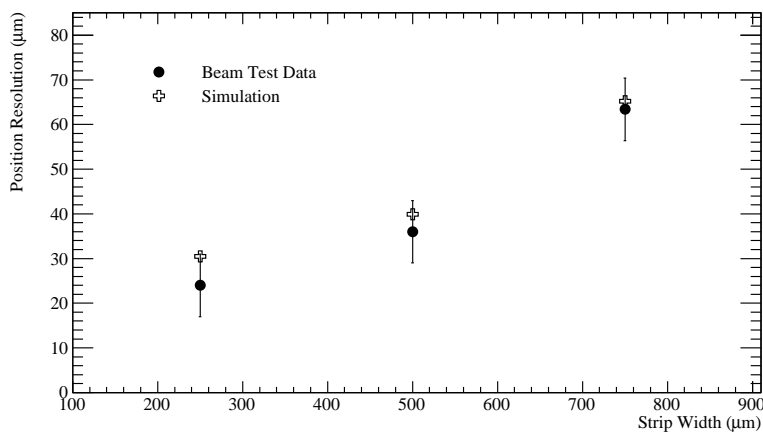

Figure 9. Measured and simulated position resolution for the 2008 beam test as a function of the strip width. The uncertainties attributed to the different experimental points are correlated.

5 Micromegas as μ-TPC

To overcome the dependence of the position resolution on the incidence angle [18] several strategies could be followed. In case enough space is available, one could tilt the chambers in order to minimize the mean incidence angle [19]. Alternatively, the gas gap width could be decreased to the absolutely operational minimum, albeit with possible effect on the reconstruction efficiency. Another method would be to use the Micromegas as a — micro — Time Projection Chamber (μ-TPC) where the few millimeter drift gap plays the role of the drift volume in a traditional TPC.

The principle of operation of the μ-TPC [20, 21] is presented in figure 11. The arrival time of the ionization clusters on the strips can be used to reconstruct the trajectory, slope and intercept, of the track in the drift gap. The longer the projection of the path length, the more effective this approach will be for a given strip width. The reconstruction of the local track direction can be advantageous for pattern recognition, even at the trigger level.
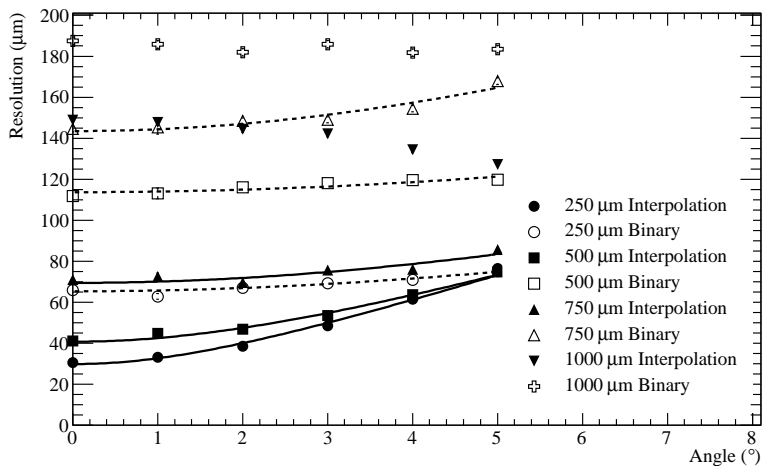
Figure 10. Spatial resolution for charge interpolation and binary read-out as a function of the incidence angle and strip width. The lines, where available, are fits to the formula $\sigma = \sigma_0 \oplus \sigma_\theta \tan\theta$, where σ_0 the resolution for perpendicular tracks, θ the incidence angle and σ_θ a parameter related to the properties of the sensitive material [18].
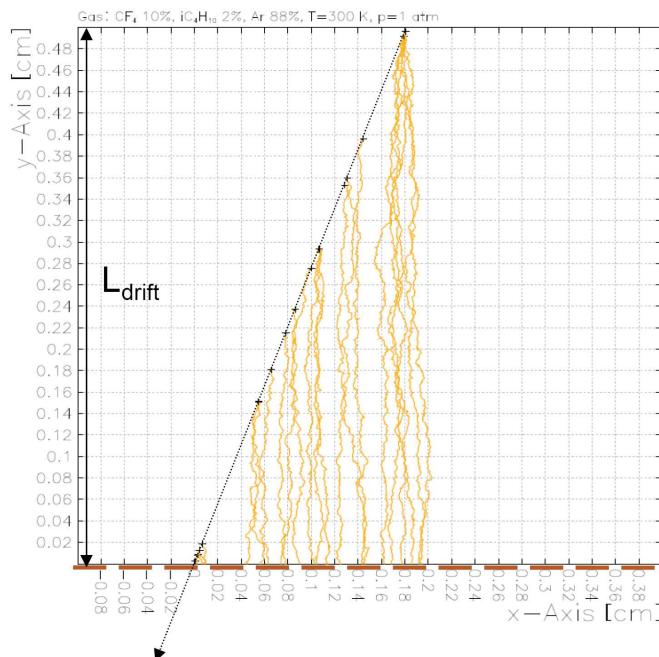

Figure 11. Principle of operation of the μ-TPC. The dotted arrow denotes the incident muon track, the crosses on the track path are the ionization clusters and the yellow lines are the drift paths of the individual electrons.

One of the major factors for the successful application of the μ-TPC method is the time resolution, which should be of the order of few ns. In the 2008 beam test data, the long integration time of the preamplifier and the jitter of the trigger with respect to the ALTRO clock, did not permit an in-depth study of this method. However, an exploratory study has been pursued: The drift time

information for each strip was extracted from the peak time of the signal pulse. The earliest peak time was used as the timing reference. By converting these drift times to drift distances, measurement points were formed subsequently fitted to a line. One significant source of uncertainty is the fluctuations in the spatial distribution of the primary ionization clusters along the track path. Additionally, electrons drifting longer will be more affected by diffusion. From the available data it is suggested that for a gas gap of 5 mm and a strip pitch of 500 μm, the direction of a track inclined by 35° could be measured with 11% resolution.

The μ-TPC method is a very interesting approach to overcome the angle dependence of the position resolution. At the same time it is a very challenging one, since the requirements for the μ-TPC method are almost perpendicular to those for charge interpolation methods.

6 Future directions

During the summer of 2009, a half-size prototype with active area 400 mm × 1300 mm was under preparation at CERN, by CERN/EN-ICE. It will be equipped with a calendered mesh of stainless-steel wires. The pitch of the wires is 56.4 μm, while their diameter is 18 μm. The amplification gap is 128 μm and the mesh is segmented into six parts. Two strip widths were selected, 250 and 500 μm, while the length of the strips is 350 and 800 mm. It will be conditioned and characterised with laboratory tests as soon as it becomes available and it will be tested in one of the forthcoming beam test periods.

The parallel plate geometry of the Micromegas detector makes it susceptible to discharges. Given the abundance of neutrons and photons in the ATLAS environment, it is very important to minimize the dead-time of the chamber and keep it at acceptable levels. Currently, two main approaches to resolve this issue are followed: a) use resistive coating on the read-out strips; and b) double stage amplification. In order to assess the severity of this issue, and the effectiveness of the suggested solutions, irradiation tests in neutron facilities using smaller size chambers will be performed.

As soon as the materials to be used for the chamber construction are defined, extensive ageing tests will be performed to ensure the good operation of the chamber in the harsh environment of the LHC.

7 Summary

The ten-fold luminosity increase in the s-LHC will require an upgrade of the ATLAS Muon Spectrometer in order to maintain its good performance. The use of bulk-Micromegas for this upgrade is proposed and a dedicated R&D programme with this aim was launched in 2007. A medium-size prototype has been prepared and tested in a pion beam showing good performance in terms of operation stability, gas amplification, efficiency and spatial resolution for perpendicular tracks. Simulation software that will ease performance studies has been developed and its results were found in agreement with the beam test data. Interesting approaches to overcome the angle dependence of the position resolution and the discharge rate are being pursued. The R&D activity is on-going with the construction of a half-size detector (400 mm × 1300 mm), gas mixture optimization and detailed studies of the detector performance — for example the time resolution.

Acknowledgments

References

[1] ATLAS collaboration, *ATLAS detector and physics performance: technical design report, 1*, CERN-LHCC-99-014 (1999); *ATLAS detector and physics performance: technical design report, 2*, CERN-LHCC-99-015 (1999).

[2] ATLAS collaboration, G. Aad et al., *The ATLAS Experiment at the CERN Large Hadron Collider*, 2008 *JINST* **3** S08003.

[3] O. Brüning et al., *LHC design report. I. The LHC main ring*, CERN-2004-003-V-1 (2004).

[4] ATLAS collaboration, A. Airapetian et al., *ATLAS muon spectrometer: technical design report*, CERN-LHCC-97-022 (1997).

[5] S. Baranov et al., *Estimation of Radiation Background, Impact on Detectors, Activation and Shielding Optimization in ATLAS*, CERN-ATL-GEN-2005-001 (2005).

[6] Y. Giomataris, P. Rebourgeard, J.P. Robert and G. Charpak, *MICROMEGAS: a high-granularity position-sensitive gaseous detector for high particle-flux environments*, *Nucl. Instrum. Meth.* **A 376** (1996) 29.

[7] G. Barouch et al., *Development of a fast gaseous detector "Micromegas"*, *Nucl. Instrum. Meth.* **A 423** (1999) 32.

[8] I. Giomataris et al., *Micromegas in a bulk*, *Nucl. Instrum. Meth.* **A 560** (2006) 405 [physics/0501003].

[9] H. Müller et al., *Development of muon chambers based on Micromegas technology for the upgrade of the ATLAS experiment for the SLHC*, submitted to *IEEE Trans. Nucl. Sci.*.

[10] ALICE collaboration, H. Müller et al., *Configurable electronics with low noise and 14-bit dynamic range for photodiode-based photon detectors*, *Nucl. Instrum. Meth.* **A 565** (2006) 768.

[11] R. Esteve Bosch, A. Jimenez de Parga, B. Mota and L. Musa, *The ALTRO chip: a 16-channel A/D converter and digital processor for gas detectors*, *IEEE Trans. Nucl. Sci.* **50** (2003) 2460.

[12] ALICE collaboration, C.W. Fabjan et al., *ALICE trigger data-acquisition high-level trigger and control system: technical design report*, CERN-LHCC-2003-062 (2004).

[13] J. Treis et al., *A modular PC based silicon microstrip beam telescope with high speed data acquisition*, *Nucl. Instrum. Meth.* **A 490** (2002) 112 [physics/0210004].

[14] R. Veenhof, *GARFIELD, recent developments*, *Nucl. Instrum. Meth.* **A 419** (1998) 726.

[15] I.B. Smirnov, *Modeling of ionization produced by fast charged particles in gases*, *Nucl. Instrum. Meth.* **A 554** (2005) 474.

[16] S.F. Biagi, *Monte Carlo simulation of electron drift and diffusion in counting gases under the influence of electric and magnetic fields*, *Nucl. Instrum. Meth.* **A 421** (1999) 234.

[17] E. Mathieson and G.C. Smith, *Charge distributions in parallel plate avalanche chambers*,
Nucl. Instrum. Meth. **A 273** (1988) 518.

[18] P. Rehak and E. Gatti, *Semiconductor detectors in nuclear and particle physics*,
AIP Conf. Proc. **338** (1995) 319.

[19] T. Argyropoulos et al., *Cathode strip chambers in ATLAS: installation, commissioning and in situ
performance*, *IEEE Trans. Nucl. Sci.* **56** (2009) 1568.

[20] T. Bressani, G. Charpak, D. Rahm and Č. Zupančič, *Track localization by means of a drift chamber*, in
proceedings of *Dubna Meeting on Filmless and Streamer Chambers*, Dubna Russia, April 15–18 1969.

[21] B. Peyaud, *KABES: a novel beam spectrometer for NA48*, *Nucl. Instrum. Meth.* **A 535** (2004) 247.